Vibrational hyperpolarizabilities and the Kerr effect in CH_4, CF_4, and SF_6

D. P. Shelton and J. J. Palubinskas
Physics Department, University of Nevada, Las Vegas, Las Vegas, Nevada 89154

(Received 31 July 1995; accepted 6 November 1995)

The hyperpolarizabilities γ of CH_4, CF_4, and SF_6 were measured by the dc Kerr effect at wavelengths from 457.9 to 1092 nm. Vibrational hyperpolarizabilities γ^v were obtained by combining these measurements with electric-field-induced second harmonic generation (ESHG) measurements. The vibrational contribution to the hyperpolarizability ranges from 6% to 35% of the total. At high optical frequency the difference between γ^v for Kerr and γ^v for ESHG is approximately constant, and has values 18, 31, and 51×10^{-63} $C^4\,m^4\,J^{-3}$ for CH_4, CF_4, and SF_6, respectively. The experimental results are in good quantitative agreement with the results of recent *ab initio* calculations of the frequency dependence of γ^v for CH_4, except for a small but non-negligible discrepancy at high frequency. © *1996 American Institute of Physics.* [S0021-9606(96)00207-9]

I. INTRODUCTION

There has been much recent theoretical and experimental interest in the nonlinear optical (NLO) properties of materials.[1–3] The motivation for these studies ranges from the testing of *ab initio* calculations of molecular properties, to the development of materials suitable for NLO device applications. A wide range of NLO effects are mediated by the molecular hyperpolarizabilities (which also play a role in intermolecular interactions). The hyperpolarizabilities of a given order for a particular molecule are all intimately related, being instances of a single function which depends on the electric field oscillation frequencies and polarizations. The relationship between the second hyperpolarizabilities γ for different NLO processes is one focus of this work.

Here we present dc Kerr effect (electric-field-induced birefringence) measurements of the hyperpolarizability $\gamma(-\nu;0,0,\nu)$ at several optical frequencies ν, which are compared with previous electric-field-induced second harmonic generation (ESHG) measurements of $\gamma(-2\nu;\nu,\nu,0)$. The hyperpolarizability function for a particular molecule is determined by the combined electronic and nuclear motions, but it is convenient to partition γ into electronic, vibrational, and rotational contributions. The electronic hyperpolarizability γ^e, that is the hyperpolarizability in the absence of nuclear motions, has a very simple form at frequencies far below the first electronic resonance. The dispersion function for the *zzzz* or $\parallel$ component of the orientationally averaged electronic hyperpolarizability γ^e is given by

$$\gamma^e_{\parallel}(-\nu_\sigma;\nu_1,\nu_2,\nu_3)=\gamma^e_{\parallel}(0;0,0,0)(1+A\nu_L^2+B\nu_L^4+C\nu_L^6+\cdots), \tag{1}$$

where $\nu_\sigma=\Sigma_i\nu_i$ and $\nu_L^2=\nu_\sigma^2+\nu_1^2+\nu_2^2+\nu_3^2$ (e.g., $\nu_L^2=2\nu^2$ for the dc Kerr effect and $\nu_L^2=6\nu^2$ for ESHG). The coefficients A and B are the same for dc Kerr and ESHG,[4] so $\gamma^e_{\parallel}$ vs ν_L^2 for the two processes will follow the same dispersion curve at frequencies low enough that the $C\nu_L^6$ and higher terms are small. This is the case for all the measurements considered here.

The nuclei as well as the electrons move in response to the applied electric fields, and the vibrational hyperpolarizability γ^v accounts for the effect of the nuclear vibrational motions. In the static limit, γ^v is comparable to or even much larger than γ^e in magnitude. The frequency dependence of γ^v is more complicated than that of γ^e because the range of vibrational resonance frequencies usually overlaps the range of the relevant oscillation frequencies (the applied field frequencies, their harmonics, and their sums and differences). The magnitude of γ^v can be quite different for different NLO processes, and there is a tendency for γ^v to be larger when the NLO process involves applied static fields. Recently there has been developed a theoretical method which is suitable for the calculation of γ^v as a function of frequency for polyatomic molecules,[5] but as yet there are few experimental results with which to test these calculations.

In these experiments we have chosen the molecules CH_4, CF_4, and SF_6 because there is no rotational hyperpolarizability contribution γ^R to complicate the measurements and analysis for spherical-top molecules. Comparison of the Kerr results with accurate, already available ESHG data is expected to provide a good measure of γ^v, and these measurements will be used to test a recent calculation of γ^v for CH_4.[6] This sort of treatment was first carried out by Elliott and Ward.[7] The accumulation of experimental hyperpolarizability data and progress with the computation of vibrational hyperpolarizabilities during the intervening decade now allows us to push the treatment much further.

II. EXPERIMENTAL METHOD

The apparatus and techniques for gas-phase dc Kerr measurements with nanoradian sensitivity and 0.1% accuracy have been previously described.[8–10] The gas Kerr cell (GKC) is placed between crossed polarizers and is probed by a laser beam. The experiment measures the birefringence induced in the gas sample placed between plane parallel electrodes in the GKC, when an electric potential difference is applied between the electrodes. The retardation ϕ induced in

 0021-9606/96/104(7)/2482/6/$10.00

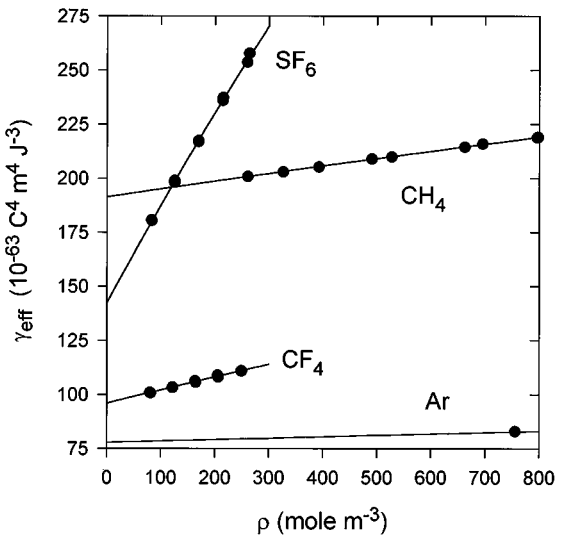

FIG. 1. The effective hyperpolarizability measured by the dc Kerr effect increases as the gas sample density is increased, due to intermolecular interactions. For each gas, two sets of five data points taken at $\lambda=632.8$ nm and $T=23$ °C on different days are shown, along with the fitted curve used for the zero density extrapolation. The argon data extends to 4500 mol m^{-3}.

the GKC is calibrated by comparison with the retardation induced in a liquid Kerr cell (LKC) containing CS_2, also placed between the crossed polarizers. The LKC is absolutely calibrated by comparing its effect with the effect of rotation of the analyzing polarizer. The effective hyperpolarizability of the sample molecules is given in terms of the known geometry of the apparatus and the measured signals S, voltages V, and sample density ρ, by[9]

$$\gamma^K_{\rm eff}=L_0^{-2}L_\nu^{-2}\,\frac{3\epsilon_0\lambda_0 d^2}{\pi D}\,\frac{F_L K_L}{\rho}\,\frac{V_L^{(0)}V_L^{(\omega)}}{V_G^{(0)}V_G^{(\omega)}}\,\frac{S_G^{(\omega)}}{S_L^{(\omega)}}, \tag{2}$$

where $L_\nu=(n_\nu^2+2)/3$ is the Lorentz local field factor for gas of refractive index n_ν, ν is the light frequency, and λ_0 is the light wavelength in vacuum, d and D are the GKC electrode spacing and effective length, $F_L K_L$ is the LKC calibration factor, and ω is the ac modulation frequency. Because there are strong intermolecular interaction effects, $\gamma^K_{\rm eff}$ is measured over a range of sample densities and extrapolated to zero density to obtain γ. Figure 1 shows typical measurements made at $\lambda=632.8$ nm.

Measurements were made over the range $\lambda=457.9$–1092 nm using several lasers (Ar^+, 457.9, 488.0, 514.5, 1092 nm; He–Ne, 632.8 nm; dye, 589.0, 763.5 nm) with a typical beam power at the sample of 3 mW. Except at 1092 nm, where the electro-optic stabilizer could not be used, the measurements of the retardation were at the shot-noise-limit of about ± 1 nrad. The GKC retardation was in the range 100–3000 nrad for samples with densities in the range 80–4500 mol/m^3. All measurements were made at about $T=23$ °C. Gas densities were determined from the measured pressure and temperature using the virial equation of state,[11] and local field factors were evaluated using tabulated refractive indices.[12] The reproducibility of $\gamma^K_{\rm eff}$ measurements at $\lambda=632.8$ nm for CH_4, made over a span of several years during which time the apparatus was completely disassembled, was $\pm 0.2\%$.

Since there are inconsistent results in the literature for the dc Kerr effect,[13–16] special care was taken to understand and eliminate systematic error sources in these experiments. Our apparatus operates over a wide wavelength range by eliminating the usual quarter-wave-plate, at the expense of making the LKC calibration very sensitive to uncompensated stray retardation. Our techniques are adequate to keep potential systematic errors due to this source below the 0.1% level, and the uncertainties due to the other quantities appearing in Eq. (2) are also readily assessed and controlled. Another important source of systematic errors and irreproducibility in the dc Kerr measurements is the extreme sensitivity to sample contamination. The Kerr effect is much stronger for anisotropic and dipolar molecules. For example, the Kerr effect for CO_2 is 30 times larger than for CF_4, and for CH_3Cl it is 800 times larger. Just a few parts per million of impurities such as CH_3Cl could significantly alter the experimental results. High purity gases were used (minimum purity 99.999%, 99.97%, 99.95%, and 99.93% by volume for Ar, CH_4, CF_4, and SF_6, respectively), and before filling with the sample gas, the GKC was subjected to an extended bake-out under vacuum to reduce outgassing from the cell walls. The typical impurities in the source gases do not have large Kerr constants, and introduction of high Kerr constant contaminants was carefully avoided. The maximum errors due to gas impurities are 0.01%, 0.3%, 0.2%, and 0.1% for Ar, CH_4, CF_4, and SF_6, respectively. Kerr measurements were made for Ar gas as a check.

III. EXPERIMENTAL RESULTS

The hyperpolarizability is obtained by fitting

$$\gamma^K_{\rm eff}=a+b\rho+c\rho^2 \tag{3}$$

to the Kerr data, where the zero-density intercept is $\gamma^K=a$. The three-body interaction term $c\rho^2$ makes a small but significant contribution to the fitted value of γ^K, but the density range of the present measurements is too small to accurately determine c. Therefore, the value of c has been constrained using information from collision-induced light scattering (CILS) measurements.[17] The intensity of the depolarized scattered light from a low density gas of spherical-top molecules is due to the polarizability anisotropy of pairs and triplets of interacting molecules, and is just proportional to $b\rho^2+c\rho^3$. The values of c in our fits have been constrained using the ratios c/b determined from CILS measurements, shown in Table I. The values of b/a obtained from the constrained fits in this work agree with the values obtained in previous work, also shown in Table I, except in the case of argon. The discrepancy in b/a for argon is due to the truncation of the fitting function at the $b\rho$ term in the previous work. The measured value of b varies slowly with wavelength. On the basis of the dipole-induced-dipole model one predicts that $b\propto\alpha(0)^2\alpha(\nu)^2$, so that b is expected to vary with wavelength due to the dispersion of the polarizability

TABLE I. Coefficients of the virial expansion $\gamma_{\text{eff}}=a+b\rho+c\rho^2$ describing the density dependence of dc Kerr measurements, obtained from several sources, are compared. Unless otherwise indicated the results are for γ=632.8 nm.

Molecule	Density range (mol m^{-3})[a]	b/a (10^{-5} m^3 mol^{-1})		c/b (10^{-5} m^3 mol^{-1})	
		Kerr[a]	Kerr	CILS[b]	Kerr[c]
Ar	750–4500	8.9±0.3	7.5±1.2[d] 6.3±1.2[c,f]	−6.1±0.3	
CH_4	260–800	19.6±0.2	24±3[c] 18±2[e]	−8.2±0.6	−12±9
CF_4	80–260	65±2	63±13[c] 54±10[e]	−12±1	−5±5
SF_6	80–270	328±4	273±43[d] 540±114[c,f]	−28±4	−21±13

[a]The present work.
[b]Reference 17; λ=488.0 nm.
[c]Reference 15.
[d]Reference 13.
[e]Reference 14.
[f]λ=457.9 nm.

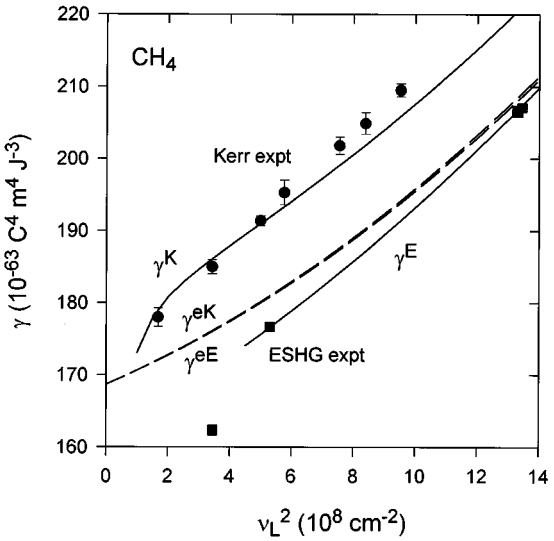

FIG. 2. Hyperpolarizabilities vs frequency are shown for CH_4. Circles and squares are dc Kerr and ESHG measurements, respectively. The error bars on the ESHG measurements are smaller than the plotted symbols (typically less than ±0.5%). The lower solid curve is a fit of Eq. (1) to the ESHG data (see Table III). The lowest frequency ESHG data point is excluded from the fit because of resonance with a nearby vibrational overtone, but the fitted curve passes through the remaining 13 ESHG data points over the range $\nu_L^2=5-27\times10^8$ cm^{-2}. The other curves, labeled γ^{eE}, γ^{eK}, and γ^K, are calculated by combining ESHG experimental results with *ab initio* results for γ^v, as explained later in the text. Note that the curves for γ^{eK} and γ^{eE} are almost indistinguishable.

α.[13,15] The expected increases in $b\propto\alpha^2$ from λ=633 nm to 458 nm are 3.5%, 1.8%, and 1.6% for CH_4, CF_4, and SF_6, respectively,[12] consistent with the corresponding observed increases, 1±6%, 6±5%, and 2±6%.

The results for γ^K obtained by extrapolating the present data to zero density are given in Table II, along with results of previous measurements. The present and previous results are in agreement, except for the results of Dunmur *et al.*[15] which fall about 20% low. The assigned error bars on the present results are from 0.4% to 3.5%. The most extensive and accurate data was taken at λ=632.8 nm. The stated error bars include both statistical uncertainties and an estimate of systematic errors.

IV. ANALYSIS AND DISCUSSION

The results of these Kerr measurements and the previous ESHG measurements[18] are both plotted vs ν_L^2 in Figs. 2, 3, and 4 for CH_4, CF_4, and SF_6, respectively. Recalling Eq. (1), one sees that γ^e will follow a single curve for each gas, so the difference between the Kerr and ESHG dispersion curves is due to the vibrational hyperpolarizability γ^v. The γ^K curves run roughly parallel to and about 6%–50% above the γ^E curves. Thus, γ^v is nearly frequency independent and is 6%–50% as large as γ^e at optical frequencies for these molecules. This qualitative behavior agrees with the theoretical expectation that γ^v tends to a constant in the high frequency limit.

The detailed comparison of dc Kerr and ESHG results is

TABLE II. Hyperpolarizabilities measured by the dc Kerr effect.

λ_{air} (nm)	ν_{vac} (cm^{-1})	γ^K (10^{-63} C^4 m^4 J^{-3})							
		Ar		CH_4		CF_4		SF_6	
		present	previous	present	previous	present	previous	present	previous
1 092	9 152			178.0±1.3		93.7±1.3		142±5	
763.5	13 094			185.0±1.0					
632.8	15 798	77.8±0.6	73±5[a]	191.4±0.7	180±9[b]	96.1±0.4	93±5[b] 77±5[c]	142.4±0.8	146±13[a]
589.0	16 973			195.3±1.7					
514.5	19 430		75.5±2.2[d]	201.8±1.2		98.8±0.6		148±4	
488.0	20 487			204.9±1.5					
457.9	21 831		74±6[c]	209.5±0.9	192±10[c]	100.4±0.5	77±15[c]	152±5	119±8[c]

[a]Reference 13.
[b]Reference 14.
[c]Reference 15.
[d]Reference 16.

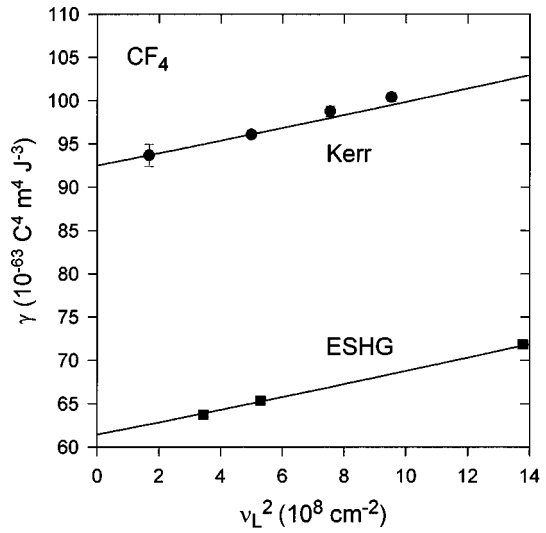

FIG. 3. Hyperpolarizabilities versus frequency are shown for CF_4. Circles and squares are dc Kerr and ESHG measurements, respectively. The error bars on the ESHG measurements are smaller than the plotted symbols (typically less than $\pm 0.5\%$). The lower curve is a fit of Eq. (1) to 9 ESHG data points over the range $\nu_L^2 = 3\text{–}26\times 10^8$ cm^{-2} (see Table III), while the upper curve is obtained by a parallel displacement.

slightly more complicated because the quantity actually measured in the Kerr experiment is a combination of tensor components $\gamma^K = 3/2\ (\gamma_\parallel - \gamma_\perp)^K$ rather than just $\gamma_\parallel^K$, where $\perp$ denotes the $zxxz$ component of orientationally averaged γ. In the static limit $\gamma_\parallel/\gamma_\perp = 3$ and $\gamma^K = \gamma_\parallel^K$, but at optical frequencies these relations are only approximate because of small deviations from Kleinman symmetry. The deviation of γ^e from Kleinman symmetry follows a dispersion relation

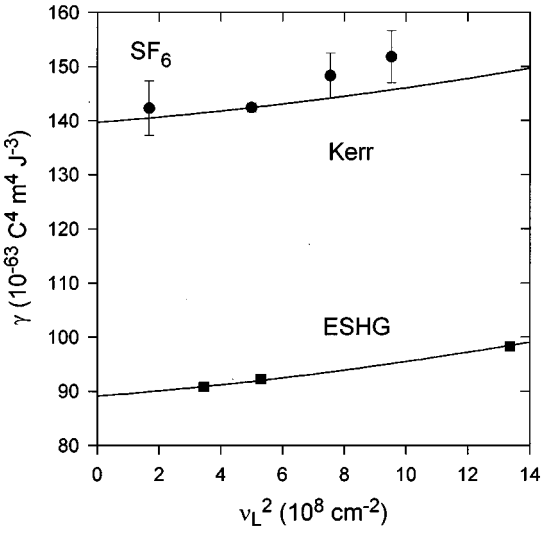

FIG. 4. Hyperpolarizabilities versus frequency are shown for SF_6. Circles and squares are dc Kerr and ESHG measurements, respectively. The error bars on the ESHG measurements are smaller than the plotted symbols (typically less than $\pm 0.5\%$). The lower curve is a fit of Eq. (1) to 8 ESHG data points over the range $\nu_L^2 = 3\text{–}29\times 10^8$ cm^{-2} (see Table III), while the upper curve is obtained by a parallel displacement.

TABLE III. Coefficients of the dispersion curves obtained by fitting Eq. (1) and Eq. (4) to the ESHG experimental results for Ar, CH_4, CF_4, and SF_6 in Refs. 18 and 19.

Molecule	γ^E (10^{-63} C^4 m^4 J^{-3})	A (10^{-10} cm^2)	B (10^{-20} cm^2)	A^{E*} (10^{-12} cm^2)
Ar	72.75	1.066	2.033	-0.1 ± 0.3
CH_4	161.5	1.532	4.334	-3.3 ± 0.3
CF_4	61.4	1.145	0.498	-0.5 ± 0.5
SF_6	89.1	0.500	2.124	$+1.6\pm 0.5$

$$\gamma_\parallel^e/\gamma_\perp^e = 3(1 + A^*\nu_L^2 + \cdots), \tag{4}$$

where theory predicts $A^{K*} = -A^{E*}$.[4] The results of ESHG measurements[19] of A^{E*} are shown in Table III, along with the coefficients of the dispersion curves[18] fitted to the ESHG data for $\gamma_\parallel^E$. The electronic hyperpolarizabilities γ^{eK} for the Kerr effect can be estimated using the expression

$$\gamma^{eK} = (3/2)(\gamma_\parallel - \gamma_\perp)^{eK} = \gamma_\parallel^{eE}[1 - (1/2)A^{E*}\nu_L^2]. \tag{5}$$

For Ar, where γ is entirely electronic and the deviations from Kleinman symmetry are essentially negligible, one finds agreement between the Kerr result $\gamma^{eK} = 77.8\pm 0.6\times 10^{-63}$ C^4 m^4 J^{-3} from this work and the ESHG result $\gamma^{eE} = 77.0\pm 0.4\times 10^{-63}$ C^4 m^4 J^{-3} from the fitted dispersion curve, at the common value of $\nu_L^2 = 4.9915\times 10^8$ cm^{-2}. This comparison for Ar serves as a check for systematic errors in the dc Kerr measurements and also as a check of the theoretical relations between γ^{eK} and γ^{eE}.

Recent *ab initio* calculations of γ^v for polyatomic molecules (NH_3, H_2O, CO_2) at optical frequencies show that either γ^{vK} or γ^{vE} can be larger depending on the particular molecule,[20] contrary to the notion that γ^v simply increases as the number of zero field frequencies involved in the NLO process.[7] In the case of CH_4, the combination of extensive experimental Kerr and ESHG data and the recent calculations of γ^v by Bishop and Pipin[6] allows us to make a fairly complete analysis of the relations between the two NLO processes and to test the theoretical calculations of γ^v.

Figure 5 shows the calculated γ^{vK} and γ^{vE} dispersion curves for CH_4. The calculated values of γ^v can be represented as a simple series in inverse powers of ν_L^2 for $\nu > 8700$ cm^{-1}, but at lower frequencies γ^v has a more complicated frequency dependence due to the resonances at molecular vibration frequencies. The calculated static value of γ^v for CH_4 is 55.25×10^{-63} C^4 m^4 J^{-3}. The γ^{eE} dispersion curve shown in Fig. 2 is obtained by subtracting calculated γ^{vE} from measured γ^E and fitting a power series in ν_L^2 to the result. A simple power series in ν_L^2 will be valid down to $\nu = 0$ for γ^{eE} but not for γ^E. The γ^{eK} dispersion curve in Fig. 2 is obtained from γ^{eE} by means of Eq. (5). Finally, the γ^K dispersion curve is obtained by adding γ^{eK} to γ^{vK}.

The calculated dispersion curve for γ^K of CH_4, shown in Fig. 2, passes close to the experimental measurements but not through all the error bars. The discrepancy is 30% of γ^{vK} at the highest frequency. The experimental value for the difference $(\gamma^K - \gamma^E)$, evaluated directly from the Kerr data

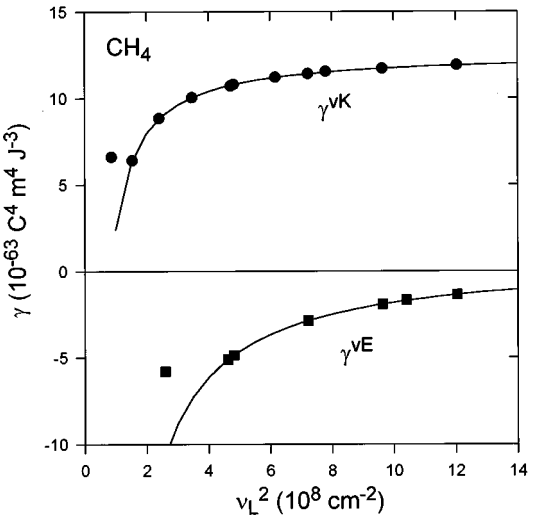

FIG. 5. The circles and squares are *ab initio* values of $\gamma^{\nu K}$ and $\gamma^{\nu E}$ for CH_4 calculated by Bishop and Pipin (Ref. 6) plotted vs frequency. The curves are fits to the points for $\nu > 8700$ cm^{-1}. The upper fitted curve is $\gamma^{\nu K} = 12.60 - 8.309\ \nu_L^{-2} - 1.868\ \nu_L^{-4}$ and the lower fitted curve is $\gamma^{\nu E} = 0.7347 - 24.22\ \nu_L^{-2} - 13.07\ \nu_L^{-4}$, with units $\gamma^{\nu}(10^{-63}\ C^4\,m^4\,J^{-3})$ and $\nu_L^2(10^8\ cm^{-2})$.

points and the fit to the ESHG data points, increases with frequency and levels off at $18 \pm 1 \times 10^{-63}$ $C^4\,m^4\,J^{-3}$ at the highest measurement frequency. In contrast, the *ab initio* result for $(\gamma^K - \gamma^E) = (\gamma^{\nu K} - \gamma^{\nu E})$ decreases with frequency and reaches a constant value 12×10^{-63} $C^4\,m^4\,J^{-3}$ in the high frequency limit.[6] Experiment and theory disagree as to the size of $(\gamma^{\nu K} - \gamma^{\nu E})$ as well as its ν_L^2 dependence.

There are several possible explanations for the discrepancy. A problem with the experimental measurements is that the ESHG data are sparse in the ν_L^2 range of the Kerr measurements. While there are 14 ESHG data points, all but two fall in the range $\nu_L^2 = 13 - 27 \times 10^8$ cm^{-2}, and furthermore, the lowest frequency ESHG data point (at $\lambda = 1319$ nm) is near a vibrational overtone frequency and so is expected to fall off the simple γ^E dispersion curve fitted to the higher frequency ESHG data. It is possible that the ESHG dispersion curve actually bends up in the gap between the present data points in such a way that the calculated γ^K curve passes closer to the measured points. ESHG measurements in the $\lambda = 700$–900 nm range would address this possibility. Note that there is excellent agreement at $\lambda = 632.8$ nm where there is an ESHG measurement at an almost matching value of ν_L^2, which removes the effect of uncertainties in shape of the γ^E fitting function. Other possibilities which could account for the discrepancy are unrecognized 2% systematic errors in the highest frequency Kerr measurements, or 30% inaccuracies in the calculated vibrational hyperpolarizabilities. Such inaccuracies in the calculated values could arise because of the limitations of the present calculations, which use (a) the SCF method, which does not include electron correlation, (b) a small basis set, and (c) a theoretical expression truncated at second order in electrical and mechanical anharmonicity.

The theoretical prediction that γ^{ν} will tend to a constant value at high frequencies holds only if one ignores the dispersion of the lower order electronic properties α^e, β^e, and their derivatives with respect to the internuclear coordinates. The *ab initio* values of γ^{ν} plotted in Fig. 5 are based on the molecular property derivatives at zero frequency.[6] Since the calculations indicate that the $[\alpha^2]$ terms dominate γ^{ν} for CH_4,[6] the dispersion of α^2 should increase the calculated value of γ^{ν} by an additional 3.5% over the range $\lambda = 633$ nm to 458 nm.[12] However, the effect of the dispersion of α^2 is small, only accounting for about 1/8 of the observed discrepancy.

For CF_4 and SF_6 the values of γ^{ν} are 3 and 5 times larger, respectively, than for CH_4. The vibrational frequencies are now far below the lowest optical frequency in the measurements, and so for CF_4 and SF_6 all the ESHG data over the range $\nu_L^2 = 3 - 29 \times 10^8$ cm^{-2} fits a simple dispersion curve. Based on the assumption that γ^{ν} is constant, dispersion curves for γ^K which are parallel to the respective ESHG dispersion curves have been drawn in Figs. 3 and 4. The Kerr data falls above the parallel curves at the highest frequencies. Assuming that the $[\alpha^2]$ terms dominate γ^{ν}, one estimates that the increases in γ^{ν} due to the dispersion in α^2 over the range $\lambda = 633$–458 nm are 1.8% and 1.6% for CF_4 and SF_6,[12] consistent with the observed $3 \pm 2\%$ and $12 \pm 10\%$ increases in γ^{ν}. At $\lambda = 632.8$ nm the observed values of $(\gamma^{\nu K} - \gamma^{\nu E})$ are $31 \pm 0.5 \times 10^{-63}$ $C^4\,m^4\,J^{-3}$ and $51 \pm 0.9 \times 10^{-63}$ $C^4\,m^4\,J^{-3}$ for CF_4 and SF_6, respectively. Previous semiempirical calculations of $(\gamma^{\nu K} - \gamma^{\nu E})$ at optical frequencies gave 16×10^{-63} $C^4\,m^4\,J^{-3}$ for CF_4 (Ref. 21) and 35×10^{-63} $C^4\,m^4\,J^{-3}$ for SF_6,[22] in rough agreement with the observed values. These calculations indicate that $\gamma^{\nu K}$ and $\gamma^{\nu E}$ at high frequency have the same sign, and that $|\gamma^{\nu K}| > |\gamma^{\nu E}|$ for CF_4 but $|\gamma^{\nu K}| < |\gamma^{\nu E}|$ for SF_6. However, these semiempirical results may be unreliable because the cancellation of terms makes them sensitive to imperfections in the input data and flaws in the calculation. A reliable partition of $(\gamma^{\nu K} - \gamma^{\nu E})$ into $\gamma^{\nu K}$ and $\gamma^{\nu E}$ awaits accurate *ab initio* calculations.

In conclusion, these experiments measure vibrational hyperpolarizabilities which are 6%–50% of the size of the electronic hyperpolarizabilities at optical frequencies for small polyatomic molecules. The size of γ^{ν} increases as the molecular size increases and as the molecular vibration frequencies decrease. The experimental results are in good quantitative agreement with the results of the recent *ab initio* calculations of the frequency dependence of γ^{ν} for CH_4, except for a small but non-negligible discrepancy at high frequency. Discovery of the reason for the difference is made difficult in the case of CH_4 because high frequency vibrational resonances complicate the dispersion curves, and because the entire vibrational contribution is only 6% of the total hyperpolarizability. In contrast, the Kerr and ESHG dispersion curves for CF_4 are simple and γ^{ν} is a large fraction of γ, so the experimental data for CF_4 should provide a critical quantitative test of *ab initio* calculations of γ^{ν} for this molecule.

ACKNOWLEDGMENT

We thank Professor David Bishop for providing the results of his work prior to publication.

[1] Chem. Rev. Thematic Issue on Optical Nonlinearities in Chemistry, edited by D. M. Burland, **94**(1) (1994).
[2] Adv. Chem. Phys. Issue on Modern Nonlinear Optics, edited by M. Evans and S. Kielich, **85** (1993).
[3] Int. J. Quantum Chem. Special Issue on Molecular Nonlinear Optics, edited by M. A. Ratner, **43**(1) (1992).
[4] D. M. Bishop, J. Chem. Phys. **90**, 3192 (1989).
[5] D. M. Bishop and B. Kirtman, J. Chem. Phys. **95**, 2646 (1991); **97**, 5255 (1992).
[6] D. M. Bishop and J. Pipin, J. Chem. Phys. **103**, 4980 (1995).
[7] D. S. Elliott and J. F. Ward, Mol. Phys. **51**, 45 (1984).
[8] D. P. Shelton and R. E. Cameron, Rev. Sci. Instrum. **59**, 430 (1988).
[9] D. P. Shelton, Rev. Sci. Instrum. **64**, 917 (1993).
[10] Refinements of the apparatus in Ref. 9 are (a) Use a windowless photodiode to eliminate a strong, disturbing position sensitivity due to etalon fringes in the window. (b) Replace MACOR ceramic insulators in the GKC with poly-ether-ether-ketone (PEEK) insulators to avoid partial electrical breakdown. (c) Match the interelectrode capacitance of the GKC and LKC using a trimmer capacitor so that the voltage divider formed by the interelectrode capacitance and the nonzero output impedance of the dc high voltage power supply does not introduce a systematic error in the ac voltage ratio determination.
[11] J. H. Dymond and E. B. Smith, *The Virial Coefficients of Pure Gases and Mixtures* (Clarendon, Oxford, 1980).
[12] *Zahlenwerte und Funktionen*, Landolt Bornstein Series, edited by K.-H. Hellwege and A. M. Hellwege (Springer, Berlin, 1962), Band II, Teil 8.
[13] A. D. Buckingham and D. A. Dunmur, Trans. Faraday Soc. **64**, 1776 (1968).
[14] A. D. Buckingham and B. J. Orr, Trans. Faraday Soc. **65**, 673 (1969).
[15] D. A. Dunmur, D. C. Hunt, and N. E. Jessup, Mol. Phys. **37**, 713 (1979).
[16] S. Carusotto, E. Iacopini, and E. Polacco, Nuovo Cimento **5D**, 328 (1985).
[17] D. P. Shelton, G. C. Tabisz, F. Barocchi, and M. Zoppi, Mol. Phys. **46**, 21 (1982); D. P. Shelton and G. C. Tabisz, *ibid*. **40**, 299 (1980).
[18] D. P. Shelton, Phys. Rev. A **42**, 2578 (1990).
[19] V. Mizrahi and D. P. Shelton, Phys. Rev. A **31**, 3145 (1985).
[20] D. M. Bishop, B. Kirtman, H. A. Kurtz, and J. E. Rice, J. Chem. Phys. **98**, 8024 (1993).
[21] Z. Lu and D. P. Shelton, J. Chem. Phys. **87**, 1967 (1987).
[22] D. P. Shelton and L. Ulivi, J. Chem. Phys. **89**, 149 (1988).